

# Change in microstructures and physical properties of $\text{ZrB}_2$ –SiC ceramics hot-pressed with a variety of SiC sources

Seongwon Kim<sup>a,\*</sup>, Jung-Min Chae<sup>a</sup>, Sung-Min Lee<sup>a</sup>, Yoon-Suk Oh<sup>a</sup>, Hyung-Tae Kim<sup>a</sup>,  
Byung-Koog Jang<sup>b</sup>

<sup>a</sup>Engineering Ceramic Center, Korea Institute of Ceramic Engineering and Technology, Icheon, Gyeonggi-do 467-843, Republic of Korea

<sup>b</sup>High Temperature Materials Unit, National Institute of Materials Science, Tsukuba 305-0047, Japan

Received 27 June 2013; received in revised form 13 September 2013; accepted 18 September 2013

Available online 30 September 2013

## Abstract

$\text{ZrB}_2$ –SiC ceramics were fabricated by hot pressing with a variety of SiC sources in order to examine the effect of the SiC size on the microstructures and physical properties, such as hardness and thermal conductivities, of  $\text{ZrB}_2$ –SiC composite ceramics. Three different  $\text{ZrB}_2$ –SiC ceramics, ZPS ( $\text{ZrB}_2$ –20 vol% polycarbosilane), ZFS ( $\text{ZrB}_2$ –20 vol% fine-grained SiC), and ZNS ( $\text{ZrB}_2$ –20 vol% nano-sized SiC), were prepared for this study. PCS is effectively transformed into  $\beta$ -SiC after hot pressing. By using PCS as a precursor for SiC,  $\text{ZrB}_2$  particles are surrounded by fine particles of SiC, which results in the grain-growth inhibition of  $\text{ZrB}_2$ . The effects of the SiC size on the microstructures and the physical properties of  $\text{ZrB}_2$ –SiC ceramics were also investigated.  $\text{ZrB}_2$ –SiC ceramics were produced by using various SiC sources in order to investigate the grain-growth inhibition and the mechanical/thermal properties of  $\text{ZrB}_2$ –SiC. The sizes of  $\text{ZrB}_2$  or SiC particles in the sintered bodies highly depend on the initial size of SiC.  $\text{ZrB}_2$ –SiC ceramics with smaller SiC show enhanced mechanical properties, consistently with the Hall–Petch relation. The thermal conductivities of  $\text{ZrB}_2$ –SiC ceramics with nano-SiC or PCS-derived SiC are higher than that of ceramics with conventional SiC, which can be explained by the percolation theory.

© 2013 Elsevier Ltd and Techna Group S.r.l. All rights reserved.

**Keywords:** C. Hardness; C. Thermal conductivity; Microstructure; SiC size;  $\text{ZrB}_2$ -based ultra-high temperature ceramics

## 1. Introduction

Among non-oxide ceramics, such as borides, carbides, and nitrides of transition metals, some compositions are categorized as ultra-high temperature ceramics [1–3]. These ceramics are a group of compounds that are chemically and physically sustainable at ultra-high temperature and in reactive atmospheres. They are also characterized by a high melting point, chemical inertness, and relatively good oxidation resistance in extreme environments including conditions experienced during hypersonic flight, atmosphere re-entry, and rocket propulsion.

$\text{ZrB}_2$  has a melting point of 3245 °C and a relatively low density of 6.1 g/cm<sup>3</sup> [4], which makes this a candidate for application to ultra-high temperature environments over

2000 °C as well as conventional applications such as electrode elements and refractory crucibles [5]. In addition to these properties,  $\text{ZrB}_2$  is known to have excellent resistance to thermal shock and oxidation relative to other non-oxide engineering ceramics [4,6]. For these purposes, it is necessary to fabricate dense body parts made of  $\text{ZrB}_2$ -based ceramics. The densification of  $\text{ZrB}_2$  powder generally requires very high temperatures due to the covalent nature of the bonding as well as its low bulk and grain boundary diffusion rates [7]. Due to these non-sinterable characteristics,  $\text{ZrB}_2$ -based ceramics have been densified by a variety of methods [4,7], including hot pressing, spark plasma sintering, reactive hot pressing, and pressureless sintering. In order to improve the oxidation resistance, SiC is frequently added to  $\text{ZrB}_2$ -based system [4,7–9]. Beside the oxidation resistance, the addition of SiC to  $\text{ZrB}_2$ -based ceramics provides enhanced mechanical properties [10,11] and thermal conductivities [12–14].

\*Corresponding author. Tel.: +82 31 645 1452; fax: +82 31 645 1492.

E-mail addresses: [woods3@kicet.re.kr](mailto:woods3@kicet.re.kr), [woods3kim@naver.com](mailto:woods3kim@naver.com) (S. Kim).

Table 1  
Compositions of the ZrB<sub>2</sub>–SiC ceramics used in this study.

ID	Composition
ZPS	ZrB <sub>2</sub> +20 vol% polycarbosilane
ZFS	ZrB <sub>2</sub> +20 vol% fine SiC (0.5 μm)
ZNS	ZrB <sub>2</sub> +20 vol% nano-SiC (< 100 nm)

Polycarbosilane (PCS) is also frequently used in ZrB<sub>2</sub>-based systems as a precursor for SiC [15] or a sintering additive for pressureless sintering [16,17].

Since the physical properties of ZrB<sub>2</sub>–SiC ceramics are closely related to the microstructure as well as the sintering additives, a thorough examination of microstructure is necessary to produce ZrB<sub>2</sub>-based ceramics with enhanced performance. In this study, ZrB<sub>2</sub>–SiC ceramics with a variety of SiC sources were investigated, in order to examine the effect of the SiC size on the microstructures and physical properties, such as hardness and thermal conductivities, of ZrB<sub>2</sub>–SiC composite ceramics.

## 2. Experimental procedure

Three different ZrB<sub>2</sub>–SiC ceramics for this study, identified as ZPS, ZFS, and ZNS, are shown Table 1. These compositions were prepared using raw powders of ZrB<sub>2</sub> (Grade F, 1.88 μm, Japan New Metals, Co. Ltd., Japan), polycarbosilane (PCS, (SiH(CH<sub>3</sub>)-CH<sub>2</sub>)<sub>n</sub>, average molecular weight ~3000, TBM Tech, Korea), fine-sized SiC (FCP 15C, 0.5 μm, SIKA Tech, Germany), and nano-sized SiC (nano powder, < 100 nm, ALDRICH, Germany). After weighing, the powders were combined by slurry mixing in acetone or isopropyl alcohol with stirring hot plate for 4 h in order to maintain the initial particle size and dried in an oven for 24 h. The dried powder mixtures were then sieved with a #120-mesh sieve for granulation. The prepared powder mixtures were hot-pressed in a graphite mold. Hot pressing was carried out at 1900 °C for 2 h under a pressure of 30 MPa in a flowing Ar atmosphere.

For hot-pressed samples, the microstructures and mechanical properties were characterized. The specimens were also ground with a diamond wheel and then polished from 6 to 1 μm of diamond slurry for microstructure analysis and hardness measurement. The microstructure was examined using field emission scanning electron microscope (FE-SEM, JSM-6701F, JEOL, Japan), and the microstructural parameters were determined by using ImageJ program [18] on SEM images of polished surfaces. Vickers hardness was also measured using a micro hardness tester (QM-2, Nikon, Japan).

Cross-sectional foils for transmission electron microscopy analysis were sliced from the polished surface of the samples using a focused ion beam (FIB, Helios 600i, FEI, USA) with a Ga ion source accelerated at 30 kV. The slices were finally thinned with a fine ion beam current to less than 100 nm, which is an electron-transparent thickness in TEM. Thin foils of the samples were examined with a transmission electron microscope (TEM, Tecnai G2 F30, FEI, USA) equipped with

an energy dispersive spectroscopy (EDS) analyzer and a high-angle annular dark-field (HAADF) detector for scanning transmission electron microscopy (STEM).

The specific heat capacities ( $C_p$ ) and thermal diffusivities ( $\lambda$ ) of the hot-pressed samples were measured by laser flash analysis (LFA, LFA 457 Micro Flash, NETZSCH, Germany) as a function of the temperature up to 1100 °C. For the measurement, both the front and back sides of the samples were coated with a thin graphite layer in order for the sample to absorb the incident laser beam and emit black-body radiation to the IR detector. The specific heat capacities were characterized from LFA by comparing the relative temperature rise of the sample with that of the reference sample of alumina. The thermal conductivity ( $K$ ) can be calculated by Eq. (1) with the apparent density ( $\rho$ ), heat capacity ( $C_p$ ), and thermal diffusivity ( $\lambda$ ).

$$K = \rho C_p \lambda \quad (1)$$

## 3. Results and discussion

### 3.1. Microstructures of PCS-derived ZrB<sub>2</sub>–SiC ceramic

Polycarbosilane (PCS) is a preceramic polymer with a Si–C backbone, frequently used in ZrB<sub>2</sub>-based systems as a precursor for SiC [15] or a sintering additive for pressureless sintering [16,17]. When pyrolyzed in an inert atmosphere, PCS forms low-molecular-weight species, which results in weight loss. As the temperature of heat treatment increases, PCS converts from amorphous products to cubic  $\beta$ -SiC with amorphous carbon. The processing parameter, such as transition temperature, ceramic yield, or C/Si ratio, is generally varies with the molecular weight of PCS. Fig. 1 shows the XRD patterns of ZrB<sub>2</sub>–20 vol% polycarbosilane (ZPS) after mixing or hot pressing and ZrB<sub>2</sub>–20 vol% SiC (ZFS) after hot pressing. As shown in Fig. 1(a), there is no other crystalline peak than ZrB<sub>2</sub> after mixing. For the XRD patterns from ZPS hot-pressed at 1900 °C (Fig. 1(b)), all of the strong peaks are from ZrB<sub>2</sub> and several very weak peaks for  $\beta$ -SiC are observed. In the case of hot-pressed ZrB<sub>2</sub>–20 vol% SiC (ZFS), the XRD peaks

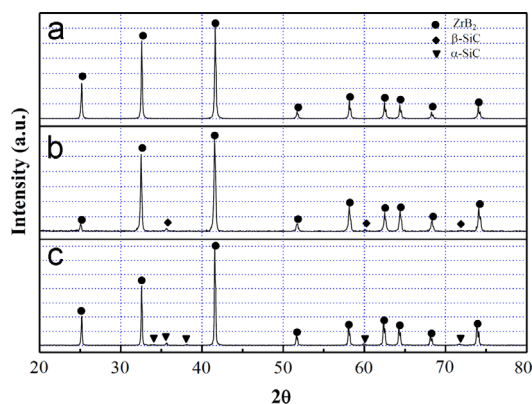


Fig. 1. XRD patterns of (a) ZrB<sub>2</sub>–20 vol% polycarbosilane (ZPS) after mixing, (b) ZrB<sub>2</sub>–20 vol% polycarbosilane (ZPS) hot-pressed at 1900 °C for 2 h, and (c) ZrB<sub>2</sub>–20 vol% SiC (ZFS) hot-pressed at 1900 °C for 2 h under 30 MPa.

from SiC correspond to those of hexagonal  $\alpha$ -SiC. Cubic SiC is usually regarded to be a low-temperature form (below  $\sim 1800^\circ\text{C}$ ) and to readily convert to an hexagonal SiC on heating to temperature in the region of  $2000^\circ\text{C}$  [19].

Fig. 2 shows an SEM micrograph of  $\text{ZrB}_2$ –20 vol% PCS (ZPS) hot-pressed at  $1900^\circ\text{C}$  for 2 h and EDS spectra from constituent phases of this microstructure. In the backscattered electron mode of SEM, grains with higher average atomic

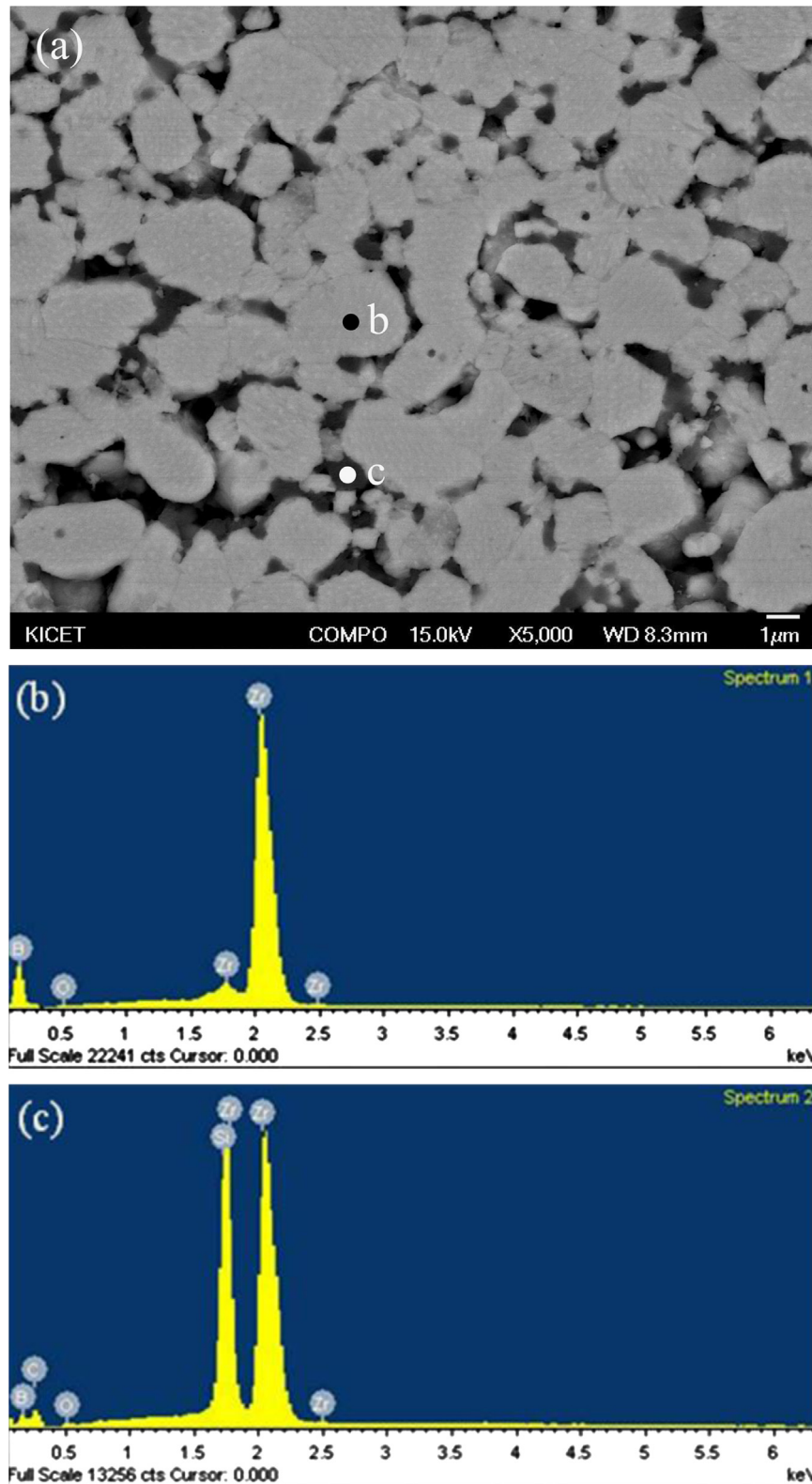


Fig. 2. (a) SEM micrographs of hot-pressed  $\text{ZrB}_2$ –20 vol% polycarbosilane (ZPS) and EDS patterns from (b) position b and (c) position c.

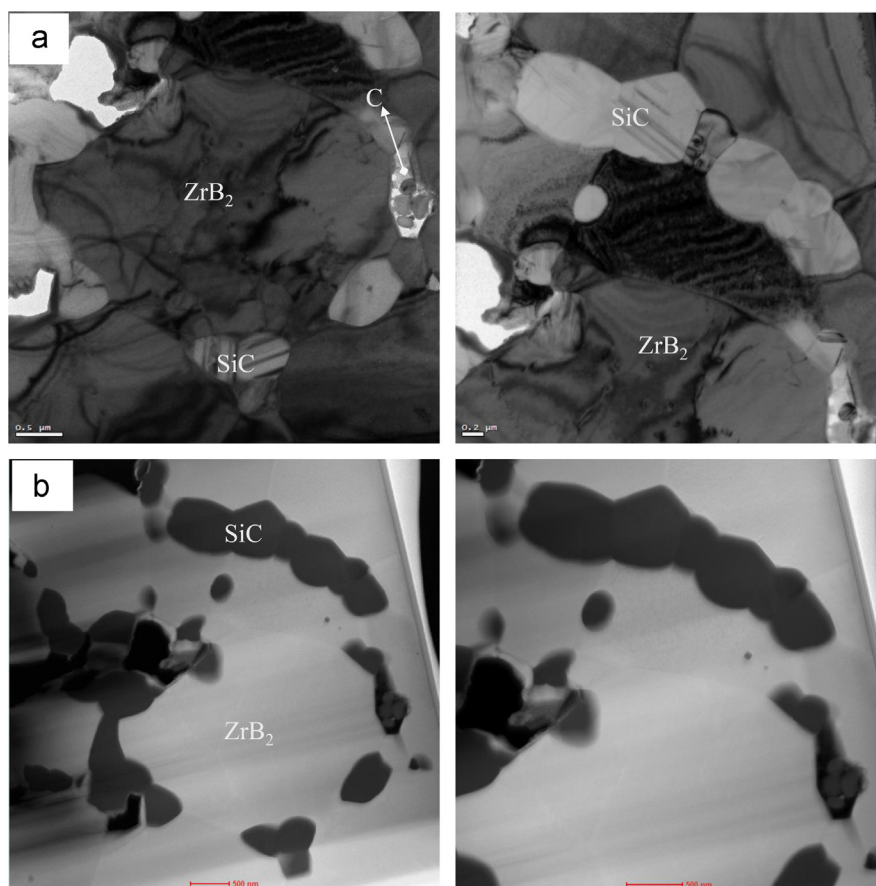


Fig. 3. Transmission electron microscopy images of hot-pressed ZrB<sub>2</sub>–20 vol% polycarbosilane (ZPS); (a) TEM bright-field images and (b) STEM/HAADF images.

weight appear in brighter contrast [20]. In the microstructure, the gray matrix round particles are ZrB<sub>2</sub>, whereas the black dispersed particles are SiC. ZrB<sub>2</sub>–SiC ceramics from PCS samples have grain-growth-inhibited ZrB<sub>2</sub> surrounded by very fine SiC particles. Moreover, the contiguity of SiC particles is significantly enhanced with the addition of PCS. Considering that the ceramic yield of PCS used in this study is about ~70%, which mainly depends on the molecular weight and pyrolysis temperature of PCS [15,16], the volume fraction of SiC in hot-pressed ZrB<sub>2</sub>–20 vol% PCS (ZPS) would be less than that of SiC in hot-pressed ZrB<sub>2</sub>–20 vol% SiC. EDS spectra confirm that the microstructure is composed of solely ZrB<sub>2</sub> and SiC. In order to examine the microstructures of hot-pressed ZPS in detail, the microstructures were characterized with transmission electron microscopy. Fig. 3 shows the TEM/STEM microstructures of ZrB<sub>2</sub>–20 vol% PCS (ZPS) hot-pressed at 1900 °C. In bright-field TEM images, diffraction contrast should be observed due to the periodicity of the atomic structure for the crystalline phases in the microstructure [21]. In contrast, amorphous phases show little contrast in bright-field images due to the absence of crystallinity. In STEM images from HAADF detector, the elemental contrast could appear like the BSE (back-scattered electron) mode [20]. Observed ZrB<sub>2</sub> or SiC is in a crystalline form, and equiaxed ZrB<sub>2</sub> grains appear to be surrounded by fine SiC grains. A

substantial amount of porosity is present near the SiC particles and amorphous carbon particles are also observed in the microstructure.

### 3.2. Microstructures and physical properties of ZrB<sub>2</sub>–SiC ceramics with a variety of SiC sources

Fig. 4 shows the SEM microstructures of ZrB<sub>2</sub>–SiC ceramics with a variety of SiC sources hot-pressed at 1900 °C for 2 h under 30 MPa pressure. As shown in Fig. 4, the size of ZrB<sub>2</sub> or SiC particles in the final microstructure definitely depends on the initial size of SiC. Measured grain sizes from the microstructures are summarized in Table 2. While the size of ZrB<sub>2</sub> is more than 10 μm in the case of fine SiC addition (ZFS), SiC particles have a size of several micrometers. For the addition of nano-size SiC (ZNS) or PCS (ZPS), ZrB<sub>2</sub> particles with several micrometer sizes, which are close to the initial particle size of ZrB<sub>2</sub>, are mainly observed in the final microstructures. The effect of second-phase particles on grain growth is known as the Zener effect [22]. If second-phase particles are present at the grain boundaries of matrix phase, these particles exert drag force against the boundary movement, which results in grain-growth inhibition. The difference in grain growth with SiC size would influence the physical properties of ZrB<sub>2</sub>–SiC.



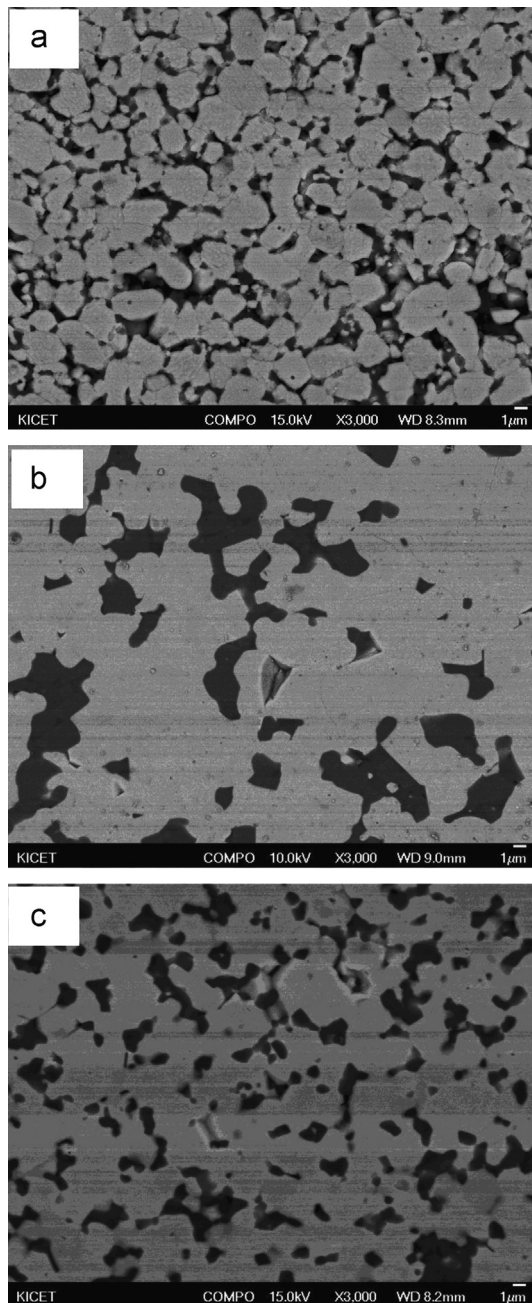


Fig. 4. SEM micrographs of (a) ZrB<sub>2</sub>-20 vol% polycarbosilane (ZPS), (b) ZrB<sub>2</sub>-20 vol% SiC (ZFS) and (c) ZrB<sub>2</sub>-20 vol% nano-SiC (ZNS) hot-pressed at 1900 °C for 2 h under 30 MPa.

Fig. 5 shows the hardness values of ZrB<sub>2</sub>-SiC ceramics at elevated temperature. The hardness values increased with a decrease in the size of ZrB<sub>2</sub> in the final microstructures. The hardness is a mechanical property, which shows the resistance to permanent plastic deformation upon applied external pressure [23]. The hardness values decrease with the testing temperature, which is attributed to the increasing tendency towards plastic deformation due to dislocation movement. The reported hardness values are 21–23 GPa for polycrystalline ZrB<sub>2</sub> but ~28 GPa for SiC [4]. Considering that the hardness of composite is determined by a rule of mixtures of each constituent phase [24], the addition of SiC results in a slight increase in hardness. The other significant factor regarding the hardness is the relationship between the grain size and the mechanical properties, expressed by the Hall–Petch relation [23]. From the results shown in Fig. 5, the hardness of ZrB<sub>2</sub>-SiC ceramics decreases in the order of ZNS > ZPS > ZFS. While the difference in hardness between ZNS and ZFS is mainly attributed to the grain size of the microstructure, the difference between ZNS and ZPS is considered to result from the volume fraction of SiC and pores.

Fig. 6 shows the specific heat capacities and thermal diffusivities of hot-pressed ZrB<sub>2</sub>-SiC with various SiC sources. There are not significant differences in specific heat capacities, since the specific heat capacities of composites generally follow the rule of mixture. On the other hand, the thermal diffusivity, one of the major components of thermal

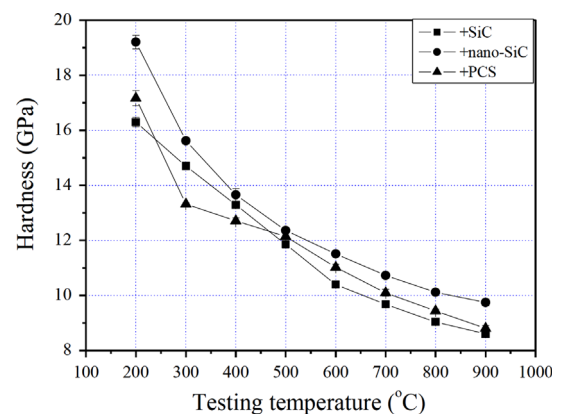


Fig. 5. Micro-Vickers hardness values as a function of the temperature of hot-pressed ZrB<sub>2</sub>-SiC ceramics with a variety of SiC sources hot-pressed at 1900 °C for 2 h under 30 MPa.

Table 2

Composition, SiC sources, apparent density, and mean size of ZrB<sub>2</sub>-SiC ceramics hot-pressed at 1900 °C for 2 h under 30 MPa.

Composition	SiC source	Apparent density (g/cm <sup>3</sup> )	Mean size(μm <sup>2</sup> )	
			ZrB <sub>2</sub>	SiC
ZPS	Polycarbosilane	5.32	2.10	0.14 (from TEM)
ZFS	Fine SiC (0.5 μm)	5.51	–	1.69
ZNS	Nano-SiC (< 100 nm)	5.51	4.27	0.62

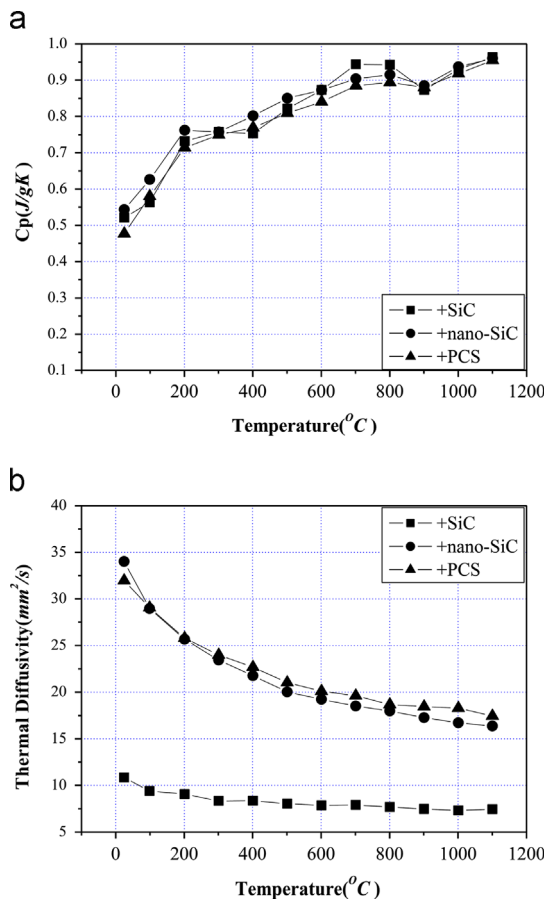


Fig. 6. (a) Specific heat capacity and (b) thermal diffusivity values as a function of temperature of hot-pressed ZrB<sub>2</sub>-SiC ceramics with a variety of SiC sources hot-pressed at 1900 °C for 2 h under 30 MPa.

conductivity, shows the percolation phenomena explained later. Even with the same volume fraction of SiC, higher thermal diffusivities are observed with the addition of nano-SiC or PCS due to the enhanced contiguity. The percolation theory can be applied to the description of conduction phenomena in ceramic composites [25]. The percolation is generally defined as the movement of fluids through porous materials. If discrepancies are present in the conductivities between the matrix and dispersed particles in composite ceramics, discrete characteristics of conductivity in composite with the volume fraction or contiguity of dispersed particles can be explained in terms of the percolation theory. One of the typical phenomena is electric conduction in composite materials between the insulating matrix and conductive dispersants [26–28]. If conductive particles are dispersed in the insulating matrix structure, the percolation threshold is referred to the minimum volume fraction of particles added to the conductive composite, which is mainly determined by insulating-to-conductive particle-size ratio. The thermal conductivity of ZrB<sub>2</sub>-SiC ceramics is also related to percolation [3,12,29]. Fig. 7 shows the calculated thermal conductivities of hot-pressed ZrB<sub>2</sub>-SiC with various SiC sources. It is obvious that ZNS or ZPS exhibits thermal conductivity values that are about twice as large as those of ZFS. The reported thermal conductivity of SiC (100–300 W/mK) [19] is larger than that of ZrB<sub>2</sub> (~60 W/mK) [4]. As shown in He's work [26], the minimum

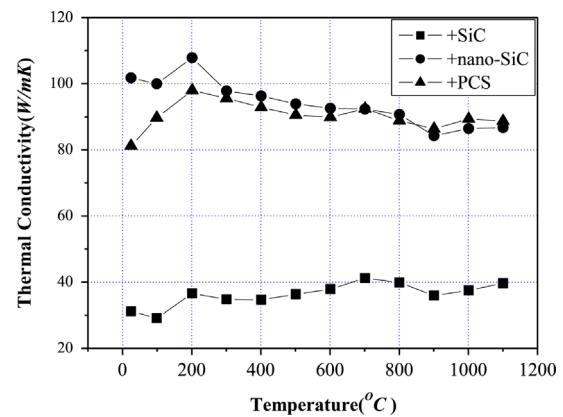


Fig. 7. Thermal conductivity values calculated as a function of temperature of hot-pressed ZrB<sub>2</sub>-SiC ceramics with a variety of SiC sources hot-pressed at 1900 °C for 2 h under 30 MPa.

volume fraction of a conducting particle in the insulating matrix, the percolation threshold, is estimated to be 0.24 for electric conduction, if the particle size of insulating particles is twice as large as that of conducting particles. This percolation threshold decreases to around 0.13 with the size ratio of 6, which means that a smaller volume fraction is necessary for electric conduction with larger size differences. In the case of thermal conduction in ZrB<sub>2</sub>-SiC, thermal conductivity close to that of SiC is attainable with the addition of smaller-sized SiC, while the volume fraction of SiC is fixed around 20 vol.%.

#### 4. Conclusions

In this study, ZrB<sub>2</sub>-SiC ceramics were fabricated by hot pressing with a variety of SiC sources in order to examine the effect of SiC size on the microstructures and physical properties, such as hardness and thermal conductivities. ZrB<sub>2</sub>-SiC ceramics are fabricated by using polycarbosilane (PCS) as a precursor for SiC. PCS is effectively transformed into  $\beta$ -SiC after hot-pressing. By using PCS as a precursor for SiC, ZrB<sub>2</sub> particles are surrounded by fine particles of SiC, which results in grain-growth inhibition of ZrB<sub>2</sub>. The effects of SiC size on the microstructures and the physical properties of ZrB<sub>2</sub>-SiC ceramics were also investigated. ZrB<sub>2</sub>-SiC ceramics were produced by using various SiC sources in order to investigate the grain-growth inhibition and the mechanical/thermal properties of ZrB<sub>2</sub>-SiC. The size of ZrB<sub>2</sub> or SiC particles in the sintered bodies highly depends on the initial size of SiC. ZrB<sub>2</sub>-SiC ceramics with nano or PCS-derived SiC show enhanced mechanical properties, consistent with the Hall-Petch relation. The thermal conductivities of ZrB<sub>2</sub>-SiC ceramics with smaller SiC are higher than that of ceramics with conventional SiC, which can be explained by the percolation theory.

#### Acknowledgments

This study was supported by a grant from “The Basic and Strategic R&D Program” funded by the Korea Institute of Ceramic Engineering and Technology, Republic of Korea.

## References

- [1] F. Monteverde, S. Guicciardi, A. Bellosi, Advances in microstructure and mechanical properties of zirconium diboride based ceramics, *Materials Science and Engineering A—Structural Materials Properties Microstructure and Processing* 346 (1–2) (2003) 310–319.
- [2] W.G. Fahrenholtz, G.E. Hilmas, A.L. Chamberlain, J.W. Zimmermann, Processing and characterization of ZrB<sub>2</sub>-based ultra-high temperature monolithic and fibrous monolithic ceramics, *Journal of Materials Science* 39 (19) (2004) 5951–5957.
- [3] M.J. Gasch, D.T. Ellerby, S.M. Johnson, Ultra high temperature ceramic composites, in: N.P. Bansal (Ed.), *Handbook of Ceramic Composite*, Kluwer Academic Publishers, Boston/Dordrecht/London, 2005, pp. 197–224.
- [4] W.G. Fahrenholtz, G.E. Hilmas, I.G. Talmy, J.A. Zaykoski, Refractory diborides of zirconium and hafnium, *Journal of the American Ceramic Society* 90 (5) (2007) 1347–1364.
- [5] S. Norasetthekul, P.T. Eubank, W.L. Bradley, B. Bozkurt, B. Stucker, Use of zirconium diboride copper as an electrode in plasma applications, *Journal of Materials Science* 34 (6) (1999) 1261–1270.
- [6] S.Q. Guo, T. Mizuguchi, M. Ikegami, Y. Kagawa, Oxidation behavior of ZrB<sub>2</sub>-MoSi<sub>2</sub>-SiC composites in air at 1500 °C, *Ceramics International* 37 (2) (2011) 585–591.
- [7] S.Q. Guo, Densification of ZrB<sub>2</sub>-based composites and their mechanical and physical properties: a review, *Journal of the European Ceramic Society* 29 (6) (2009) 995–1011.
- [8] S.S. Hwang, A.L. Vasiliev, N.P. Padture, Improved processing, and oxidation-resistance of ZrB<sub>2</sub> ultra-high temperature ceramics containing SiC nanodispersoids, *Materials Science and Engineering A—Structural Materials Properties Microstructure and Processing* 464 (1–2) (2007) 216–224.
- [9] S.Q. Guo, J.M. Yang, H. Tanaka, Y. Kagawa, Effect of thermal exposure on strength of ZrB<sub>2</sub>-based composites with nano-sized SiC particles, *Composites Science and Technology* 68 (14) (2008) 3033–3040.
- [10] F. Monteverde, Beneficial effects of an ultra-fine alpha-SiC incorporation on the sinterability and mechanical properties of ZrB<sub>2</sub>, *Applied Physics A—Materials Science and Processing* 82 (2) (2006) 329–337.
- [11] A. Rezaie, W.G. Fahrenholtz, G.E. Hilmas, Effect of hot pressing time and temperature on the microstructure and mechanical properties of ZrB<sub>2</sub>-SiC, *Journal of Materials Science* 42 (8) (2007) 2735–2744.
- [12] J.W. Zimmermann, G.E. Hilmas, W.G. Fahrenholtz, R.B. Dinwiddie, W.D. Porter, H. Wang, Thermophysical properties of ZrB<sub>2</sub> and ZrB<sub>2</sub>-SiC ceramics, *Journal of the American Ceramic Society* 91 (5) (2008) 1405–1411.
- [13] M. Ikegami, K. Matsumura, S.Q. Guo, Y. Kagawa, J.M. Yang, Effect of SiC particle dispersion on thermal properties of SiC particle-dispersed ZrB<sub>2</sub> matrix composites, *Journal of Materials Science* 45 (19) (2010) 5420–5423.
- [14] J. Zou, G.J. Zhang, H. Zhang, Z.R. Huang, J. Vleugels, O. Van der Biest, Improving high temperature properties of hot pressed ZrB<sub>2</sub>-20 vol% SiC ceramic using high purity powders, *Ceramics International* 39 (1) (2013) 871–876.
- [15] X.J. Zhou, G.J. Zhang, Y.G. Li, Y.M. Kan, P.L. Wang, Hot pressed ZrB<sub>2</sub>-SiC-C ultra high temperature ceramics with polycarbosilane as a precursor, *Materials Letters* 61 (4–5) (2007) 960–963.
- [16] S.M. Zhu, W.G. Fahrenholtz, G.E. Hilmas, Enhanced densification and mechanical properties of ZrB<sub>2</sub>-SiC processed by a preceramic polymer coating route, *Scripta Materialia* 59 (1) (2008) 123–126.
- [17] M.A. Zhu, Y.G. Wang, Pressureless sintering ZrB<sub>2</sub>-SiC ceramics at low temperatures, *Materials Letters* 63 (23) (2009) 2035–2037.
- [18] ImageJ, (<http://rsb.info.nih.gov/ij/>).
- [19] F.L. Riley, *Structural Ceramics: Fundamentals and Case Studies*, Cambridge, United Kingdom, 2009.
- [20] L.C. Feldman, J.W. Mayer, *Fundamentals of Surface and Thin Film Analysis*, Elsevier Science Publishing Co. Inc., New York, 1986.
- [21] D.B. Williams, C.B. Carter, *Transmission Electron Microscopy*, Plenum Press, New York, 1996.
- [22] S.-K.L. Kang, *Sintering: Densification, Grain Growth, And Microstructure*, Elsevier Butterworth-Heinemann, New York, 2005.
- [23] J.B. Wachtman, W.C. Cannon, M.J. Matthewson, *Mechanical Properties of Ceramics*, 2nd Ed., John Wiley & Sons, Inc., USA, 2009.
- [24] H.S. Kim, On the rule of mixtures for the hardness of particle reinforced composites, *Materials Science and Engineering A—Structural Materials Properties Microstructure and Processing* 289 (1–2) (2000) 30–33.
- [25] Y.-M. Chiang, D. Birnie III, W.D. Kingery, *Physical Ceramics*, John Wiley & Sons, Inc., New York, 1997.
- [26] D. He, N.N. Ekere, Effect of particle size ratio on the conducting percolation threshold of granular conductive-insulating composites, *Journal of Physics D—Applied Physics* 37 (13) (2004) 1848–1852.
- [27] N. Lebovka, M. Lisunova, Y.P. Mamunya, N. Vygornitskii, Scaling in percolation behaviour in conductive-insulating composites with particles of different size, *Journal of Physics D—Applied Physics* 39 (10) (2006) 2264–2271.
- [28] L. Ren, Z. Han, J. Tong, J. Li, D. Chen, D. He, Conductive percolation threshold of conductive-insulating granular composites (41, pg 2157, 2006), *Journal of Materials Science* 41 (13) (2006) 4373–4373.
- [29] M. Gasch, S. Johnson, J. Marschall, Thermal conductivity characterization of hafnium diboride-based ultra-high-temperature ceramics, *Journal of the American Ceramic Society* 91 (5) (2008) 1423–1432.